

## Feature Extraction on Range Images – A New Approach

S.A. Coleman, B.W. Scotney, S. Suganthan

**Abstract**— Range images can provide an almost 3-dimensional description of a scene. Feature driven segmentation of range images has been primarily used for 3D object recognition, and hence the accuracy of the detected features is a prominent issue. Feature extraction on range images has proven to be a more complex problem than on intensity images due to both the irregular distribution of range image data and the nature of the features that are present in range images. Approaches to range image feature extraction are often scan line based approximations that carry a significant computational overhead and hence are not appropriate for real-time processing. This paper presents a design procedure for scalable first order derivative operators that can be used directly on irregularly distributed data. Hence the method is appropriate for direct use on range image data without the requirement of image pre-processing and could form the basis of algorithms of real-time robotic applications.

### I. INTRODUCTION

IN recent years many computer vision applications have been developed that range image data instead of, or in conjunction with, intensity image data [9]. This is largely because range imagery can be used to obtain reliable descriptions of 3-D scenes; a range image contains distance measurements from a selected reference point or plane to surface points of objects within a scene [4], allowing more information about the scene to be recovered [3]. However, a range image contains information about only the visible surfaces of the objects, and not their hidden surfaces, and hence is often referred to as  $2\frac{1}{2}$ -D information [4].

One problem with range images is the extensive amount of data that is required to be stored for each individual image. This large volume of data makes direct interpretation of range images costly. To reduce the computation involved in interpreting range images, range image feature extraction and segmentation have been identified as means of scene representation and are used in applications such as object recognition [11, 16], motion analysis [18], and automated visual inspection [17]. Such segmentation techniques for range images can be generalised into two categories: region-

based segmentation, where pixels are classified into regions, and edge-based segmentation, where the region boundaries are detected. Edge-based techniques are more reliable, as region-based techniques suffer from a number of problems such as distortion of region boundaries, dependency on the initial region selection, and over-segmentation, even when applied to very simple segmentation tasks [14]. Among the research that has focussed on segmentation of range image data, there are four well-known algorithms developed in the University of South Florida [13], Washington State University [10], the University of Bern [15] and the University of Edinburgh [21]. The algorithm of [12] computes a planar fit for every pixel and then grows regions for those that have similar plane equations. The algorithm from Washington State University, which was originally developed for quadric surfaces and then modified by [10] to accept only first order surface fits, often results in oversegmented images. Jiang et al. [15] use the scan line approximation with region growing performed using a set of line segments rather than individual pixels. This algorithm is fast but does not preserve the object edges completely. Finally, [21] proposed an algorithm similar to that of [12]. Although it provides a good standard of segmentation, the method is quite slow and is sensitive to noise [14]. This paper presents feature detection methods that do not require uniform data distribution, preserving the edge localisation and hence addressing problems such as over- and under-segmentation found in the segmentation algorithms.

Whilst much research has been carried out to develop edge detection methods for range image data, little work on range data has focussed on the area of multiscale, or adaptive, edge detection methods. The requirement for scalable operators in image processing has emerged in recent years as research in the field of computer vision has shown that, typically, a feature in an image may exist significantly over a specific range of scales, with the detected strength of a feature depending on the scale at which the appropriate feature detection operator is applied. When features in an image that occur over a range of scales are extracted at only one scale, localisation error or false edges may be introduced. In order to successfully extract the various edge types found in range images, multiscale feature extraction algorithms are particularly pertinent for obtaining good feature localisation and reliability, as smooth crease edges are low-frequency events and jump edges are high-frequency events.

Due to the locational irregularity of range image data, multiscale feature detection on range images is a significantly different problem than that on intensity images. In recent work, Coleman et al., have focussed attention on

Manuscript received September 15, 2006. This work was supported in part by the U.K Research Council EPSRC under Grant EP/C006283/1.

S.A. Coleman is with the School of Computing and Intelligent Systems, University of Ulster, Londonderry, Northern Ireland. Phone: +442871375030; fax: +442871375470; e-mail: [sa.coleman@ulster.ac.uk](mailto:sa.coleman@ulster.ac.uk)

B.W. Scotney is with the School of Computing and Information Engineering, University of Ulster, Coleraine, Northern Ireland. Phone: +442870324648; e-mail: [bw.scotney@ulster.ac.uk](mailto:bw.scotney@ulster.ac.uk)

S.Suganthan is with the School of Computing and Intelligent Systems, University of Ulster, Londonderry, Northern Ireland, UK., Phone: +442871375596; e-mail: [s.suganthan@ulster.ac.uk](mailto:s.suganthan@ulster.ac.uk)

the design and implementation of scalable and adaptive first and second order derivative operators through the use of a finite element (FE) framework; such operators have been proven to perform successfully when compared with well-known intensity image feature detection operators [5, 19]. Taking advantage of the flexibility offered by the finite element method, these operators can be altered to remove the requirement for regularly located image data [6] and thus can prove to be successful for the purpose of feature extraction on range images. The framework has also been used to design and implement novel near-circular first and second order derivative operators [7, 20] that have been shown to improve edge orientation angular error. Such operators can play a key role in feature extraction for recognition, as accurate localisation of object edges is imperative.

This paper presents a brief overview of the range image representation and the design procedure for the scalable operators that we propose to use directly on the range data. Some preliminary results using first order derivative operators are presented and an overview of future work that will be carried out on the problem of directly processing range data, without any pre-processing requirements, is described.

### II. RANGE IMAGE REPRESENTATION

We consider an irregularly sampled image to be represented by a spatially irregular sample of values of a continuous function  $u(x,y)$  of depth value on a domain  $\Omega$ . Our operator design procedure is then based on the use of a quadrilateral mesh as illustrated in Fig. 1.

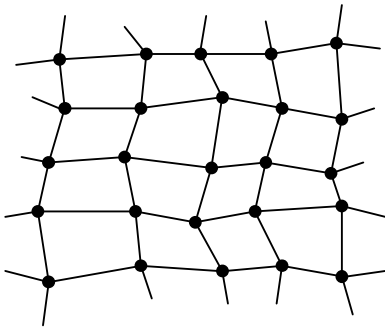


Fig. 1. Sample of the irregularly distributed range image

With each node  $i$  in the mesh is associated a piecewise bilinear basis function  $\phi_i(x, y)$  which has the properties

$$\phi_i(x_j, y_j) = \begin{cases} 1 & \text{if } i = j \\ 0 & \text{if } i \neq j \end{cases} \quad (1)$$

where  $(x_j, y_j)$  are the co-ordinates of the nodal point  $j$  in the mesh. Thus  $\phi_i(x, y)$  is a "tent-shaped" function with support restricted to a small neighbourhood centred on node  $i$  consisting of only those elements that have node  $i$  as a vertex. We then approximately represent the range image

function  $u$  by a function  $U(x, y) = \sum_{j=1}^N U_j \phi_j(x, y)$  in which the parameters  $\{U_1, \dots, U_N\}$  are mapped from the range image pixels values at the  $N$  irregularly located nodal points. Therefore, approximate image representation is a simple function (typically a low order polynomial) on each element and has the sampled intensity value  $U_j$  at node  $j$ .

### III. FINITE ELEMENT FORMULATION

We formulate image operators that correspond to weak forms of operators in the finite element method [2, 19, 20]. Operators used for smoothing may be based simply on a weak form of the image function, for which it is assumed that the image function  $u(x, y)$  belongs to the Hilbert space  $H^0(\Omega)$ ; that is, the integral  $\int_{\Omega} u^2 d\Omega$  is finite. Feature detection and enhancement operators are often based on first or second derivative approximations, for which it is necessary that the image function  $u(x, y)$  is constrained to belong to the Hilbert space  $H^1(\Omega)$ ; i.e. the integral  $\int_{\Omega} (|\nabla u|^2 + u^2) d\Omega$  is finite, where  $\nabla u$  is the vector  $(\partial u / \partial x, \partial u / \partial y)^T$ .

Corresponding to a first directional derivative  $\partial u / \partial b \equiv \underline{b} \cdot \nabla u$  we may use a test function  $v \in H^1(\Omega)$  to define the weak form

$$E(u) = \int_{\Omega} \underline{b} \cdot \nabla u v d\Omega \quad (2)$$

Here  $\underline{b} = (\cos \theta, \sin \theta)$  is the unit direction vector.

In the finite element method a finite-dimensional subspace  $S^h \subset H^1$  is used for function approximation; in our design procedure the irregular image  $U$  is a function in  $S^h$ , and  $S^h$  is defined by the irregular quadrilateral mesh of elements and piecewise bilinear basis functions described in Section 2.

Since we are focusing on the development of operators that can explicitly embrace the concept of size and shape, our design procedure uses a finite-dimensional test space  $T_{\sigma}^h \subset H^1$  that explicitly embodies a size parameter  $\sigma$  that is determined by the local scatter point density. This generalisation allows sets of test functions  $\psi_i^{\sigma}(x, y)$ ,  $i=1, \dots, N$ , to be used when defining irregular derivative based operators; for first order operators, this provides the functional

$$E_i^{\sigma}(U) = \int_{\Omega_i^{\sigma}} \underline{b}_i \cdot \nabla U \psi_i^{\sigma} d\Omega_i \quad (3)$$

For the test space  $T_\sigma^h$  a set of Gaussian basis functions is used that explicitly embodies the scale parameter  $\sigma$ . The use of these basis functions within the finite element framework enables the development of operators appropriate for use on irregular image data. Sets of Gaussian test functions  $\psi_i^\sigma(x, y)$ ,  $i=1, \dots, N$  of the form

$$\psi_i^\sigma(x, y) = \frac{1}{2\pi\sigma^2} e^{-\left(\frac{(x-x_i)^2+(y-y_i)^2}{2\sigma^2}\right)} \quad (4)$$

are constructed, each restricted to have support over a neighbourhood  $\Omega_i^\sigma$  centred on the node  $i$  at  $(x_i, y_i)$ . The size of the neighbourhood  $\Omega_i^\sigma$  to which the support of  $\psi_i^\sigma(x, y)$  is restricted is also explicitly related to the scale parameter  $\sigma$  [8]. Here, the neighbourhood  $\Omega_i^\sigma$  is defined to have a real-valued "radius"  $W_\sigma^{e_m}$  for each quadrilateral element  $e_m$  in  $\Omega_i^\sigma$ . In each case  $W_\sigma^{e_m}$  is chosen as the diagonal of the element from the operator centre  $(x_i, y_i)$ . The test function  $\psi_i^\sigma$  is therefore comprised of a set of sectors of Gaussian functions  $\psi_i^{\sigma_m}$ , where  $\psi_i^{\sigma_m}$  is the test function over element  $e_m$  in  $\Omega_i^\sigma$ . In each case choosing the element scale parameter  $\sigma_m = W_\sigma^{e_m} / 1.96$  ensures that the diagonal of element  $e_m$  through  $(x_i, y_i)$  encompasses 95% of the cross-section of the Gaussian.

IV. ELEMENT-BY-ELEMENT COMPUTATION

We illustrate the approach applied to first derivative approximation using an irregular bilinear quadrilateral discretisation formed from a set of quadrilateral elements such as that illustrated in Fig. 1. We construct a set of basis functions  $\phi_i(x, y)$ ,  $i=1, \dots, N$ , so that the  $N$ -dimensional image subspace  $S^h$  comprised of functions that are piecewise bilinear.

On a neighbourhood  $\Omega_i^\sigma$  we consider a locally constant unit vector  $\underline{b}_i = (b_{i1}, b_{i2})^T$  where  $b_{i1}^2 + b_{i2}^2 = 1$ . Substituting the image representation  $U(x, y) = \sum_{j=1}^N U_j \phi_j(x, y)$  into the weak form  $E_i^\sigma(U) = \int_{\Omega_i^\sigma} \underline{b}_i \cdot \nabla U \psi_i^\sigma d\Omega_i$  gives

$$E_i^\sigma(U) = b_{i1} \sum_{j=1}^N K_{ij}^\sigma U_j + b_{i2} \sum_{j=1}^N L_{ij}^\sigma U_j, \quad (5)$$

where  $K_{ij}^\sigma$  and  $L_{ij}^\sigma$  are respectively entries in  $N \times N$  global matrices  $K^\sigma$  and  $L^\sigma$  given by

$$K_{ij}^\sigma = \int_{\Omega_i^\sigma} \phi_j \frac{\partial \psi_i^\sigma}{\partial x} dx dy, \quad i, j=1, \dots, N \quad (6)$$

$$\text{and } L_{ij}^\sigma = \int_{\Omega_i^\sigma} \phi_j \frac{\partial \psi_i^\sigma}{\partial y} dx dy, \quad i, j=1, \dots, N \quad (7)$$

These integrals need be computed only over the neighbourhood  $\Omega_i^\sigma$ , rather than the entire image domain  $\Omega$ , since  $\psi_i^\sigma$  has support restricted to  $\Omega_i^\sigma$ .

Each neighbourhood  $\Omega_i^\sigma$  is composed of a set  $S_i^\sigma$  of elements. In our example implementation  $S_i^\sigma$  is the  $2W_\sigma \times 2W_\sigma$  irregular block of elements having nodal point  $(x_i, y_i)$  at its centre. We may thus write  $K_{ij}^\sigma$  and  $L_{ij}^\sigma$  as the respective summations

$$K_{ij}^\sigma = \sum_{\{m|e_m \in S_i^\sigma\}} k_{ij}^{m,\sigma} \quad \text{and} \quad L_{ij}^\sigma = \sum_{\{m|e_m \in S_i^\sigma\}} l_{ij}^{m,\sigma} \quad (8)$$

Where  $k_{ij}^{m,\sigma}$  and  $l_{ij}^{m,\sigma}$  are the *element integrals*  $k_{ij}^{m,\sigma} = \int_{e_m} \phi_j \frac{\partial \psi_i^\sigma}{\partial x} dx dy$  and  $l_{ij}^{m,\sigma} = \int_{e_m} \phi_j \frac{\partial \psi_i^\sigma}{\partial y} dx dy$ . The element integrals  $k_{ij}^{m,\sigma}$  and  $l_{ij}^{m,\sigma}$  are actually computed by mapping to the standard square element in order to facilitate the integration of the Gaussian test functions using simple quadrature rules.

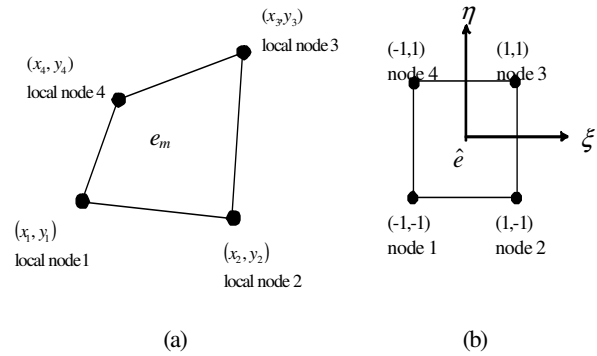


Fig. 2. (a) Cartesian reference system for Bilinear element  $e_m$  (b) Bilinear reference element.

For each element  $e_m \subset \Omega_i^\sigma$ , there are just four basis functions of the trial space  $S^h$  that have support on  $e_m$ . Following Fig. 2(a), we may denote these as  $\phi_1^m, \phi_2^m, \phi_3^m$  and  $\phi_4^m$ . A local  $(x, y)$  co-ordinate reference system for a general rectangular element  $e_m$  is introduced that may be mapped to co-ordinates  $(\xi, \eta)$  with  $-1 \leq \xi \leq 1$  and  $-1 \leq \eta \leq 1$  in the standard element  $\hat{e}$ . The co-ordinate transformation is defined as

$$x = \frac{1}{4}(x_1(1 - \xi)(1 - \eta) + x_2(1 + \xi)(1 - \eta) + x_3(1 + \xi)(1 + \eta) + x_4(1 - \xi)(1 + \eta)) \quad (9)$$

$$y = \frac{1}{4}(y_1(1 - \xi)(1 - \eta) + y_2(1 + \xi)(1 - \eta) + y_3(1 + \xi)(1 + \eta) + y_4(1 - \xi)(1 + \eta)) \quad (10)$$

In practice, integration on  $\hat{e}$  is done numerically using a low-order Gauss quadrature rule, typically requiring just four quadrature points (see [2])

Construction of the operators on an irregular quadrilateral grid differs from that of image processing operators on a typically regular grid in that it is no longer appropriate to build explicitly an entire operator, as each operator throughout an irregular mesh may be different with respect to the operator neighbourhood shape. When using an irregular grid, we work on an element-by-element basis, taking advantage of the flexibility offered by the finite element method as a means of adaptively changing the irregular operator shape to encompass the data available in any local neighbourhood. Such a local neighbourhood is illustrated by the collection of quadrilateral elements in Fig. 3; the test function  $\psi_i^\sigma$  is comprised of a set of sectors of Gaussian functions  $\psi_i^{\sigma_m}$  truncated at “radius”  $W_{\sigma^m}$ . Thus the operator is able to automatically alter its shape as required, dependent on the irregular node sampling within the range image data.

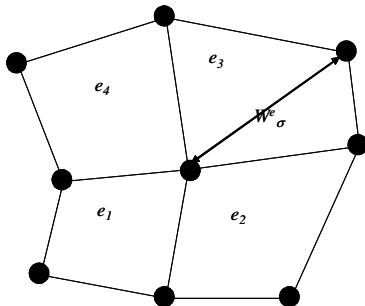


Fig. 3. Local 3x3 operator neighbourhood

V. THRESHOLDING

Here we demonstrate how thresholding differs when we apply gradient operators to range images, compared to applying such operators to intensity images. Typically with intensity images, after applying gradient operators, thresholding is applied by simply selecting an appropriate threshold value  $T$ , either empirically or scientifically, and all values that lie above  $T$  are considered as feature points. This is illustrated in Fig. 4, where if we considered the depth profile to be a sample profile from an intensity image, the slopes correspond to ramp edges and clearly, maxima in the gradient output correspond to features in an intensity image. However, if the depth profile is that of a range image, the same thresholding procedure does not provide edges when

applied to the gradient output from a range image, but instead, surfaces. Therefore in order to obtain range image features, or edges, we must identify significant changes in the gradient output.

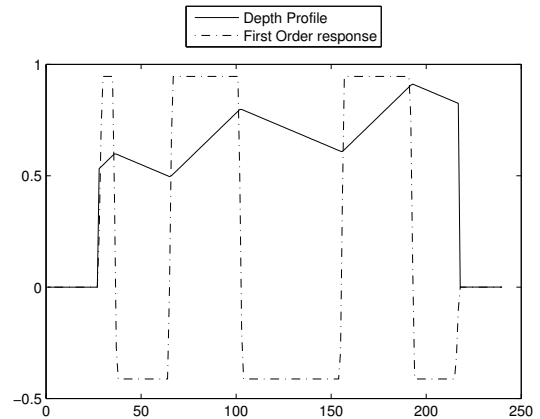


Fig.4 Sample image profile with corresponding gradient operator output

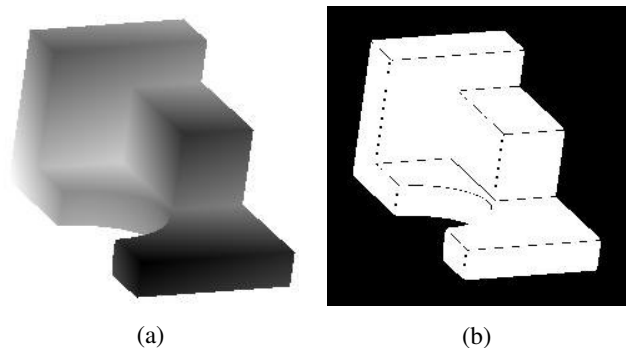


Fig. 5. (a) Original Range Image; (b) Surfaces detected using typical intensity image thresholding method

Fig. 5 illustrates the output obtained when typical intensity thresholding is applied resulting in identification of object surfaces (in white). Significant changes in gradient output can be used to identify object edges as illustrated by the results in Fig. 6.

VI. RESULTS

To demonstrate the results obtained to date, we compare our proposed technique with that of Jiang et al. [15]. The algorithm in [15] is a scan line approximation approach that scans the image vertically, horizontally and diagonally.

In Fig. 6 we show results using the Figure of Merit evaluation technique [1] for a vertical edge within a range image represented using regularly distributed data. Each Figure of Merit value is averaged over 25 images, comprising five of each range edge type: step, positive roof, negative roof, positive crease, negative crease. Various densities of salt and pepper noise were added, density ranges from 0 to 0.01. The patterns of behaviour of the two methods are similar, with the proposed technique becoming superior for lower noise densities.

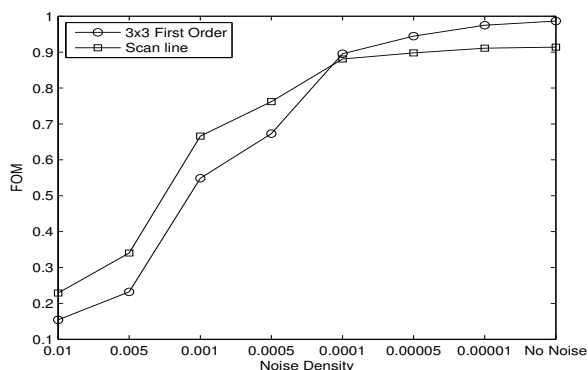


Fig 6. Figure of Merit results using a vertical edge

Feature maps for both the proposed method and that in [15] applied to the range image in Fig. 5(a) are illustrated in Fig. 7. This image is captured by the Technical Arts scanner and has regularly distributed data [22]. Here we can see that our technique provides thinner edges than that of [15] and also detects the ridges in the curve of the block.

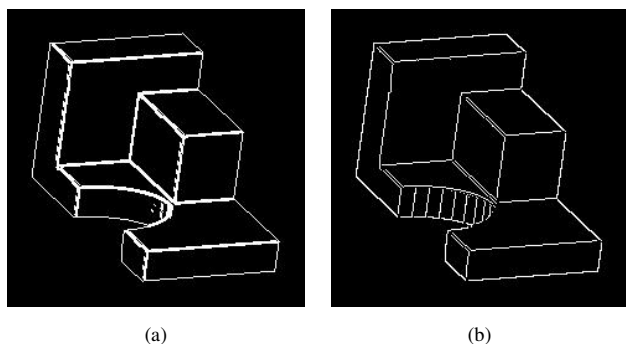


Fig. 7. (a) Feature map generated using [15]; (b) Feature map generated using proposed technique using significant gradient change thresholding

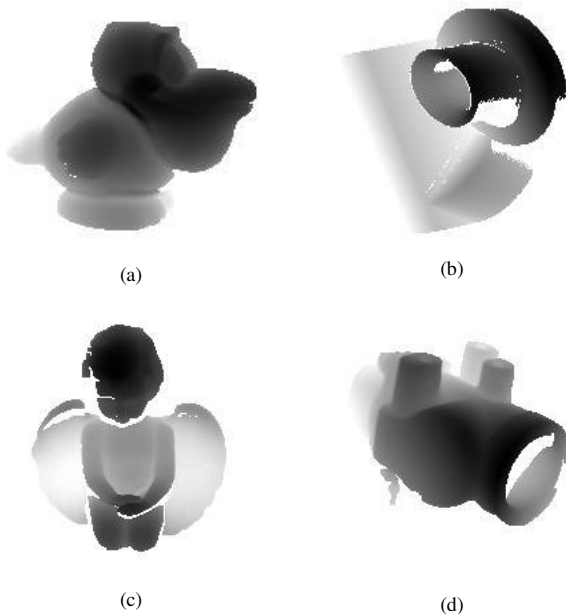


Fig. 8. Original range images from [22]

Fig. 9 illustrates the feature maps corresponding to the real range images in Fig. 8. These range images contain irregularly distributed data. Again we see that the gradient operator detected finer, more distinct features and less noise compared with the scan line approximation of [15]. It should be noted that our proposed technique automatically finds all features whereas the technique in [15] does not automatically find the object boundary via the scan line approximation but instead, in all cases, assumes the boundary at the transition between data and no data in the range image.

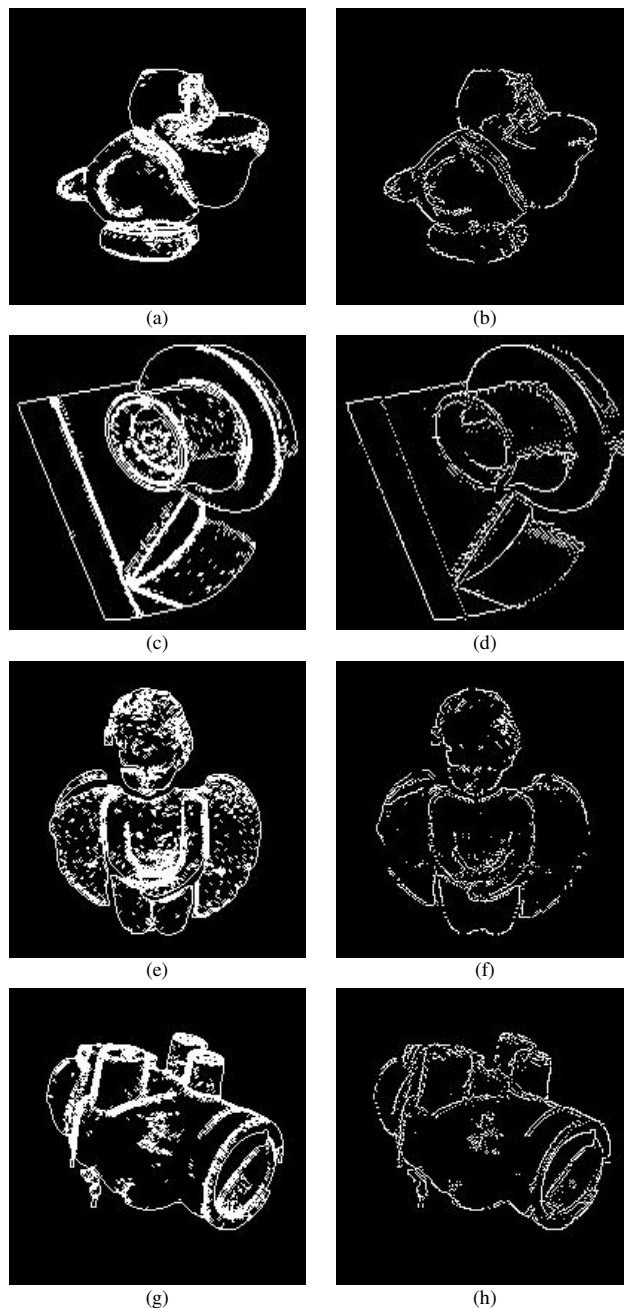


Fig. 9. (a), (c), (e), (g) Feature maps generated using [15]; (b), (d), (f), (h) Feature maps generated using proposed technique

## VII. SUMMARY AND FUTURE WORK

The overall aim of this research is to develop and implement multiscale feature extraction algorithms for direct use on irregular or incomplete range image data, improving feature localisation and enabling real-time processing for the application of robotic vision. Current results as presented in the paper in the form of first order feature maps are promising when compared with the scan line approach of Jiang et al., [15] and such techniques need to be refined and timed in order to prove their worth. Future work will involve generating irregular quadrilateral operators of varying size, not just  $3 \times 3$ . Such operators will then be adapted in order to determine the nature of the features detected: crease, jump or smooth. These techniques will be used for the purpose of segmentation and evaluated with respect to existing edge based segmentation algorithms with the overall goal of recognising objects in range images in real-time.

## ACKNOWLEDGMENT

We would like to thank Professor Horst Bunke for providing us with the code for the scan line approximation algorithm in [15].

## REFERENCES

- [1] Abdou, I. E., Pratt, W. K., "Quantitative Design and Evaluation of Enhancement/ Threshold Edge Detectors." *Proceedings of the IEEE*, Vol. 67, No. 5, May 1979
- [2] Becker, E.B., Carey, G.F., and Oden, J.T., *Finite Elements: An Introduction*, Prentice Hall, London, 1981.
- [3] Bellon, O., and Silva, L., "New Improvements on Range Image Segmentation by Edge Detection Techniques" *Proceedings of the workshop on Artificial Intelligence and Computer Vision*, Nov. 2000.
- [4] Besl, P.J., "Active, optical range imaging sensors." *Machine Vision and Apps*, Vol.1, pp127-152, 1988.
- [5] Coleman, S.A., Scotney, B.W., Herron, M.G., "Content-Adaptive Feature Extraction Using Image Variance" *Pattern Recognition, Elsevier*, Vol. 38, pp2426-2436, 2005
- [6] Coleman, S.A., Scotney, B.W. & Herron, M.G. "Image Feature Detection on Content-Based Meshes *Proc. of IEEE Int. Conf on Image Processing (ICIP2002)*, pp. 844-847
- [7] Coleman, S.A., Scotney, B.W. & Herron, M.G, "A Systematic Design Procedure for Scalable Near-Circular Laplacian of Gaussian Operators" *Proc. of Int. Conf. on Pattern Recognition (ICPR2004)*, Cambridge, pp700-703.
- [8] Davies, E.R., "Design of Optimal Gaussian Operators in Small Neighbourhoods" *Image and Vision Computing*, Vol. 5(3), 1987, 199-205.
- [9] Dias, P., et al., "Combining Intensity and Range Images for 3D Modelling", *Proceedings of the IEEE International Conference on Image Processing (ICIP2003)*.
- [10] Flynn, P.J., and Jain, A.K., "BONSAI: 3D Object Recognition Using Constrained Search" *IEEE Trans. Pattern Analysis and Machine Intelligence*, Vol 13, No. 10, pp.1066-1075, 1991.
- [11] Flynn, P.J., and Jain, A.K., "Three-dimensional object recognition" *Handbook of Pattern Recognition and Image Processing: Computer Vision*, Academic Press, San Diego, pp 497-541, 1994.
- [12] Goldgof, D.B., et al., "A Curvature-Based Approach to Terrain Recognition" *IEEE Trans. Pattern Analysis and Machine Intelligence*, Vol 11, pp.1213-1217, 1989.
- [13] Gunsel, B., et al., "Reconstruction and boundary detection of range and intensity images using multiscale MRF representations" *CVIU*, Vol. 63, pp353-366, 1996.
- [14] Hoover, A. et al., "An Experimental Comparison of Range Image Segmentation Algorithms" *IEEE Trans. Pattern Analysis and Machine Intelligence*, Vol 18, No. 7, pp.673-689, 1996.
- [15] Jiang X. Y., Bunke H. "Edge detection in range image based on scan line approximation" *Computer Vision and Image Understanding* 73(2), 183-199, 1999.
- [16] Kaveti, S., et al., "Second-Order Implicit Polynomials for segmentation of Range Images." *Pattern Recognition*, Vol. 29, No. 6, pp. 937-949, 1996.
- [17] Newman, T.S., and Jain, A.K., "A system for 3D CAD-based inspection using range images" *Pattern Recognition*, Vol. 28, No. 10, pp/ 1555-1574, 1995.
- [18] Sabata, B., and Aggarwal, J.K., "Surface correspondence and motion computation from a pair of range images", *Computer Vision and Image Understanding*, Vol. 63, pp 232-250, 1996.
- [19] Scotney, B.W., et al., "Device Space Design for Efficient Scale-Space Edge Detection." *Proc of Int. Conf. on Computational Science (ICCS2002)*. Springer-Verlag, LNCS.
- [20] Scotney, B.W., Coleman, S.A., Herron, M.G., "Improving Angular Error by Near Circular Operator Design" *Pattern Recognition, Elsevier* Vol. 37(1), pp169-172, 2004.
- [21] Trucco, E., and Fisher, R.B., "Experiments in Curvature-Based Segmentation of Range Data", *IEEE Trans. Pattern Analysis and Machine Intelligence*, Vol 17, No. 2, pp. 177-182, 1995.
- [22] <http://sampl.eng.ohio-state.edu/~sampl/data/3DDDB/RID/index.htm>